

The State and Stability of Magnesium(II) Complexes with Azaporphyrins in the Proton-Donor Medium

O. G. Khelevina, M. V. Ishutkina, and A. S. Malyasova

Ivanovo State University of Chemistry and Technology, Research Institute of Macroheterocyclic Compounds,
pr. F. Elgel'sa 7, Ivanovo, 153000 Russia
e-mail: khelevina@yandex.ru

Received July 16, 2012

Abstract—The state and stability of magnesium complexes with various azaporphyrins in the proton-donor media containing acetic acid have been studied. Kinetic parameters of the complexes dissociation have been determined, possible reactions mechanisms have been proposed.

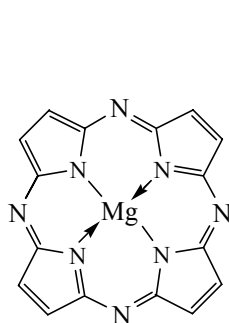
DOI: 10.1134/S1070363213080136

Chemical stabilization of azaporphyrins metal complexes is affected by the metal ion nature, ligand structure, nature of the proton-donor medium, and the complex state under the conditions of the experiment. In its complexes, magnesium forms $3s3p^33d^2$ -hybrid coordination bonds with nitrogen coordination centers, thus the complex is stabilized [1]. The MgN_4 group is planar. For example, the literature data [2] show that chlorophyll is a relatively stable complex with Mg–N coordination bonds of quite high degree of the covalent character. Magnesium complexes of azaporphyrins are bases containing electron donor centers (*meso*-nitrogen atoms) that are capable of involvement into acid-base interaction in a proton-donor medium, depending on the medium acidity. The complex stability will depend on its form, neutral or acidic, dominating under given conditions.

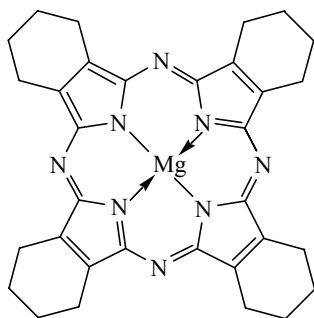
We studied the ligand structure effect on the state and stability of magnesium complexes with a series of azaporphyrins (H_2AP): 5,10,15,20-tetraazaporphyrin (H_2TAP), tetra(tetramethylene)tetraazaporphyrin ($H_2TTMTAP$), 5,7-diphenyl-1,4-diazeponitribenzoporphyrizine ($H_2Dz\cdot Bz_3Pz$), triazatetrabenzoporphyrin (H_2TATBP), and monoazatetrabenzoporphyrin (H_2MATBP) in the proton-donor media containing acetic acid.

The true (or, at constant medium acidity, effective) rate constant of the complex dissociation with the ligand elimination was taken as a measure of the complex stability. The complexes dissociation was followed at different temperatures: 30, 40, 50, and 60°C.

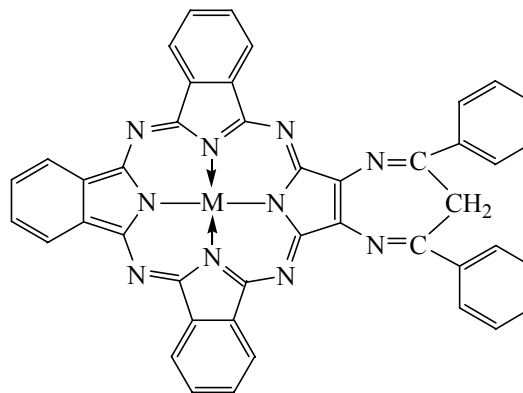
The stability of $MgTAP$, $MgTTMTAP$, and $MgTATBP$ complexes was studied in the mixture of benzene and acetic acid with addition of ethanol (4%).



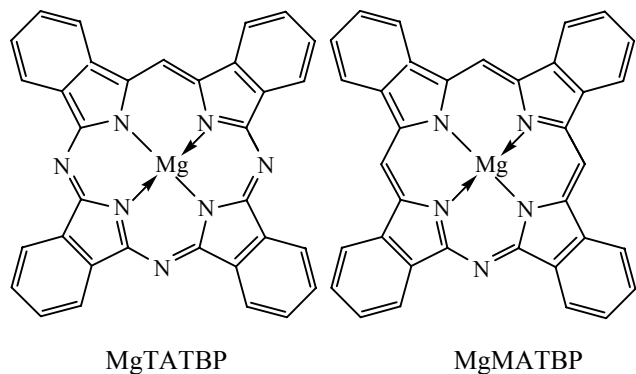
MgTAP



MgTTMTAP



MgDzBz₃Pz



The complexes dissociation occurred with the formation of the respective free ligand in the non-protonated form.



Figure 1 illustrates the changes of the complex electron absorption spectrum upon dissociation, MgTAP being a representative example. As acetic acid was taken in large excess with respect to the complex, the reaction was performed under conditions of the pseudo-first order reaction. The first order with respect to the studied complexes was confirmed by the linear shape of the $\log(c_{\text{MgAP}}^0/c_{\text{MgAP}}) = f(\tau)$ plots (c^0 and c are initial and current concentrations of the complex, respectively, τ is the reaction time) (Fig. 2). Thus, the reaction was described by the first order kinetic equation (2) with k_{ef} being the effective rate constant of the complex dissociation.

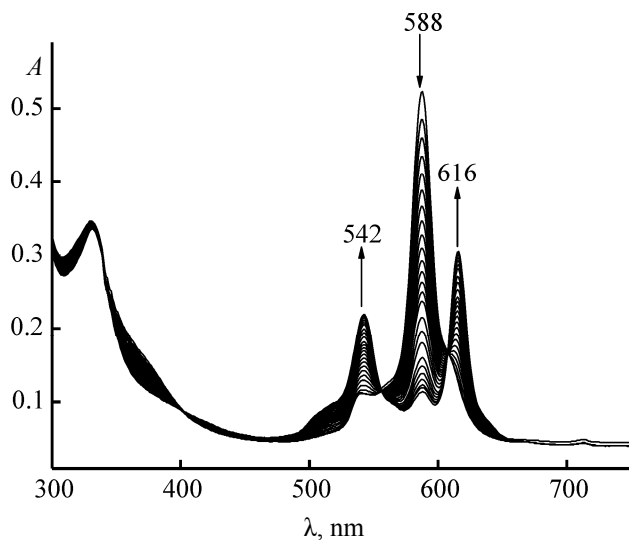


Fig. 1. Change in the electron absorption spectrum of MgTAP upon complex dissociation in the benzene – acetic acid – ethanol medium [$c(\text{CH}_3\text{COOH}) = 3.50 \text{ M}$, 323 K].

$$-dc_{\text{MgAP}}/d\tau = k_{\text{ef}}c_{\text{MgAP}}. \quad (2)$$

Kinetic parameters of the studied reactions calculated on the basis of experimental data are collected in Tables 1–3. As seen from the tables, the dissociation rate constants were dependent on the acetic acid concentration. To determine the reaction order with respect to acetic acid, the $\ln k_{\text{ef}} = f[\ln c(\text{CH}_3\text{COOH})]$ plots were analyzed. In the benzene–acetic acid–ethanol system at ethanol content below 4% the equilibrium (3) was established [1], and CH_3COOH concentration was proportional to square of $\text{C}_2\text{H}_5\text{OH}_2^+$ concentration.



Linear shape of the $\ln k_{\text{ef}} = f[\ln c(\text{CH}_3\text{COOH})]$ dependence suggested that the dissociation of MgTAP, MgTTMTAP, and MgTATBP was induced by $\text{C}_2\text{H}_5\text{OH}_2^+$, thus being a solvoprotolytic dissociation [2]. The slope of those dependences was ~ 1 (Fig. 3), so the reaction was of the second order with respect to the solvated proton, and thus it proceeded according to the trimolecular mechanism developed in [3].

The kinetic equation of the complexes dissociation was as follows Eq. (4).

$$-dc_{\text{MgAP}}/d\tau = k_v c_{\text{MgAP}} c^2(\text{C}_2\text{H}_5\text{OH}_2^+). \quad (4)$$

The experimental data revealed that the most stable complex was MgTATBP. Such substitution stabilized the complex likely due to increased rigidity and aromaticity of the macrocycle [3].

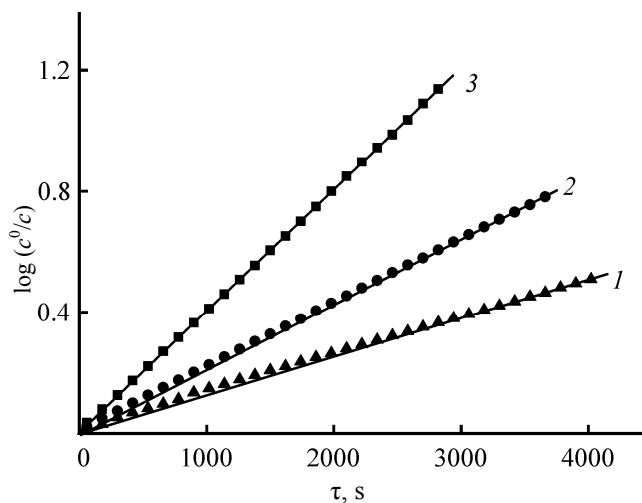


Fig. 2. $\log(c^0/c)$ as a function of time during MgTAP complex dissociation in the benzene–acetic acid–ethanol medium [$c(\text{CH}_3\text{COOH}) = 3.50 \text{ M}$]. (1) 303 K, (2) 313 K, and (3) 323 K.

Table 1. Kinetic parameters of MgTAP dissociation in the benzene–acetic acid–ethanol medium ($c_{\text{MgTAP}}^0 = 5.76 \times 10^{-6}$ M)

$c(\text{CH}_3\text{COOH})$, M	T , K	$k_{\text{ef}} \times 10^3$, s^{-1}	E , kJ mol^{-1}	ΔS^\ddagger , $\text{J mol}^{-1} \text{K}^{-1}$
0.87	298	0.02 ± 0.01^a	47 ± 4	-185 ± 6
	303	0.05 ± 0.01		
	313	0.09 ± 0.01		
	323	0.16 ± 0.02		
1.75	298	0.04 ± 0.03^a	52 ± 2	-163 ± 4
	303	0.11 ± 0.03		
	313	0.21 ± 0.02		
	323	0.40 ± 0.01		
2.62	298	0.07 ± 0.03^a	49 ± 3	-168 ± 5
	303	0.19 ± 0.02		
	313	0.34 ± 0.04		
	323	0.63 ± 0.01		
3.50	298	0.12 ± 0.04^a	46 ± 5	-174 ± 3
	303	0.30 ± 0.01		
	313	0.50 ± 0.02		
	323	0.93 ± 0.04		
4.37	298	0.13 ± 0.03^a	50 ± 2	-160 ± 6
	303	0.35 ± 0.02		
	313	0.68 ± 0.01		
	323	1.20 ± 0.03		

^a Calculated according to Arrhenius equation.

MgTAP was somewhat more stable than MgTTMTAP, even though the electron donor tetramethylene groups should have increased the covalent character of Mg–N bonds and thus the complex stability. There is no structural information about H₂TMTAP or its complexes available in the literature; our data demonstrate that tetramethylene groups are likely located out of the macrocycle plane and can thus lead to the macrocycle distortion and the Mg complex destabilization.

The stability of MgTTMTAP complex was also studied in the benzene–acetic acid medium in the absence of ethanol. In this medium the complex existed in the protonated form. Its dissociation proceeded with the formation of the ligand in the non-protonated form.

The reaction was carried out in the large excess of acetic acid, under conditions of the pseudo-first order reaction, thus, kinetic equation (2) was applied. The respective kinetic parameters are listed in Table 4. In the nonpolar aprotic solvent the complex dissociation occurred due to interaction with acetic acid molecules, thus, it was the case of acidoprotolytic dissociation. It

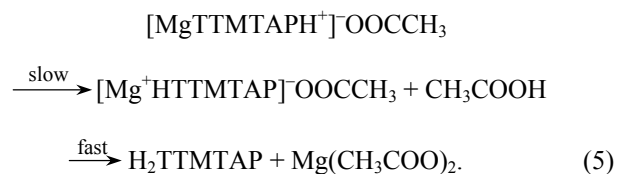
Table 2. Kinetic parameters of MgTTMTAP dissociation in the benzene–acetic acid–ethanol medium ($c_{\text{MgTTMTAP}}^0 = 8.44 \times 10^{-6}$ M)

$c(\text{CH}_3\text{COOH})$, M	T , K	$k_{\text{ef}} \times 10^3$, s^{-1}	E , kJ mol^{-1}	ΔS^\ddagger , $\text{J mol}^{-1} \text{K}^{-1}$
0.87	298	0.11 ± 0.02^a	21 ± 6	-260 ± 10
	303	0.15 ± 0.01		
	313	0.22 ± 0.04		
	323	0.25 ± 0.01		
1.045	298	0.12 ± 0.01^a	20 ± 5	-261 ± 12
	303	0.17 ± 0.04		
	313	0.24 ± 0.03		
	323	0.28 ± 0.03		
1.31	298	0.13 ± 0.08^a	32 ± 4	-225 ± 10
	303	0.18 ± 0.01		
	313	0.29 ± 0.04		
	323	0.39 ± 0.07		
1.485	298	0.17 ± 0.03^a	26 ± 2	-238 ± 9
	303	0.29 ± 0.06		
	313	0.40 ± 0.05		
	323	0.55 ± 0.07		

^a Calculated according to Arrhenius equation.

was revealed that the effective rate constant of MgTTMTAP dissociation was independent of the acetic acid concentration, and the slope of the linear plots $\ln k_{\text{ef}} = f[\ln c(\text{CH}_3\text{COOH})]$ was zero. Such result has never been reported before.

The mechanism of the acidoprotolytic dissociation is as follows. In the first stage (fast) acetic acid protonated the *meso*-nitrogen atom. In the second stage (slow), the intramolecular proton transfer from the *meso*-nitrogen atom to the endocyclic nitrogen atom of the MgN₄ group and the rupture of one of the Mg–N bonds occurred. The subsequent attack of CH₃COOH molecule leads to the fast rupture of the second Mg–N and to the formation of the free ligand. CH₃COO[−] anions coordinated to Mg cation.



MgTTMTAP dissociation in the benzene–acetic acid medium was approximately twice as fast as in the presence of ethanol, because the axial coordination of alcohol molecules impeded the solvated proton attack due to steric hindrance. Moreover, the complexes

Table 3. Kinetic parameters of MgTATBP dissociation in the benzene–acetic acid–ethanol medium ($c_{\text{MgTATBP}}^0 = 5.39 \times 10^{-6}$ M)

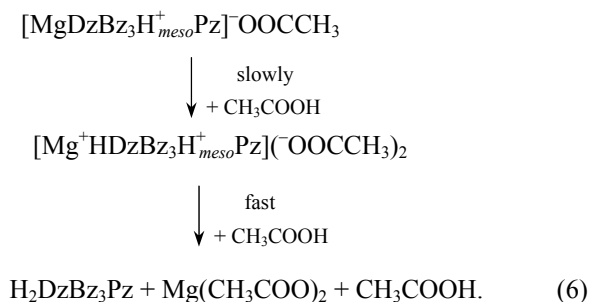
$c(\text{CH}_3\text{COOH})$, M	T , K	$k_{\text{ef}} \times 10^3$, s^{-1}	E , kJ mol^{-1}	ΔS^\ddagger , $\text{J mol}^{-1} \text{K}^{-1}$
0.87	298	0.15 ± 0.01^a	39 ± 6	$-254 \pm$
	313	0.31 ± 0.04		
	323	0.57 ± 0.04		
	333	0.77 ± 0.02		
	333	0.77 ± 0.02		
1.31	298	0.20 ± 0.03^a	42 ± 6	-202 ± 8
	313	0.41 ± 0.02		
	323	0.83 ± 0.03		
	333	1.10 ± 0.04		
	333	1.10 ± 0.04		
1.75	298	0.27 ± 0.04^a	48 ± 2	-180 ± 4
	313	0.69 ± 0.03		
	323	1.20 ± 0.03		
	333	2.10 ± 0.04		
	333	2.10 ± 0.04		
2.185	298	0.37 ± 0.01^a	44 ± 1	-190 ± 3
	313	0.87 ± 0.02		
	323	1.50 ± 0.05		
	333	2.40 ± 0.04		
	333	2.40 ± 0.04		
2.62	298	0.59 ± 0.02^a	43 ± 5	-190 ± 10
	313	1.30 ± 0.02		
	323	2.50 ± 0.04		
	333	3.50 ± 0.05		
	333	3.50 ± 0.05		

^a Calculated according to Arrhenius equation.

protonation decreased their stability due to weakening of the Mg–N bonds.

In the benzene–acetic acid medium, the *meso*-nitrogen atom of MgDzBz₃Pz was protonated [4]. The complex dissociation in this medium was acidoprotolytic as well, and proceeded with the formation of the non-protonated ligand (Fig. 4). The slope of linear plot $\ln k_{\text{ef}} = f[\ln c(\text{CH}_3\text{COOH})]$ was ~ 1 (Fig. 5, Table 5). Thus, in the case of MgDzBz₃Pz dissociation one molecule of acetic acid participated in the rate-limiting stage of the reaction.

We suggest the following scheme of MgDzBz₃Pz dissociation [Eq. (6)].

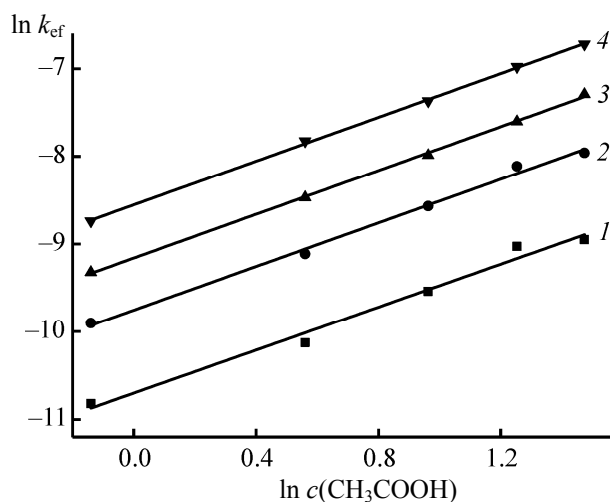
**Table 4.** Kinetic parameters of MgTTMTAP dissociation in the benzene–acetic acid medium ($c_{\text{MgTTMTAP}}^0 = 8.44 \times 10^{-6}$ M)

$c(\text{CH}_3\text{COOH})$, M	T , K	$k_{\text{ef}} \times 10^3$, s^{-1}	E , kJ mol^{-1}	ΔS^\ddagger , $\text{J mol}^{-1} \text{K}^{-1}$
0.44	298	0.22 ± 0.02^a	48 ± 2	-164 ± 4
	303	0.56 ± 0.02		
	313	1.02 ± 0.01		
	323	1.81 ± 0.03		
	323	1.81 ± 0.03		
0.87	298	0.22 ± 0.02^a	50 ± 4	-156 ± 6
	303	0.56 ± 0.03		
	313	1.10 ± 0.02		
	323	1.92 ± 0.03		
	323	1.92 ± 0.03		
1.31	298	0.22 ± 0.02^a	50 ± 1	-155 ± 1
	303	0.57 ± 0.02		
	313	1.12 ± 0.02		
	323	2.00 ± 0.04		
	323	2.00 ± 0.04		
1.75	298	0.22 ± 0.02^a	50 ± 2	-157 ± 5
	303	0.58 ± 0.03		
	313	1.11 ± 0.03		
	323	2.02 ± 0.02		
	323	2.02 ± 0.02		

^a Calculated according to Arrhenius equation.

The intramolecular proton transfer did not occur in the case of MgDzBz₃Pz, likely due to higher basicity of the *meso*-nitrogen atoms. To support this assumption, we have studied the state of H₂TTMTAP in the CH₂Cl₂–CF₃COOH medium.

Figure 6 illustrates the spectral changes during titration of the porphyrazine dissolved in dichloromethane with trifluoroacetic acid, CF₃COOH concentration being in the range of 3×10^{-4} – 1.3×10^{-2} M.

**Fig. 3.** Dependence of $\ln k_{\text{ef}}$ on $\ln c(\text{CH}_3\text{COOH})$ in the case of MgTAP dissociation at different temperatures: (1) 298 K, (2) 303 K, (3) 313 K, and (4) 323 K.

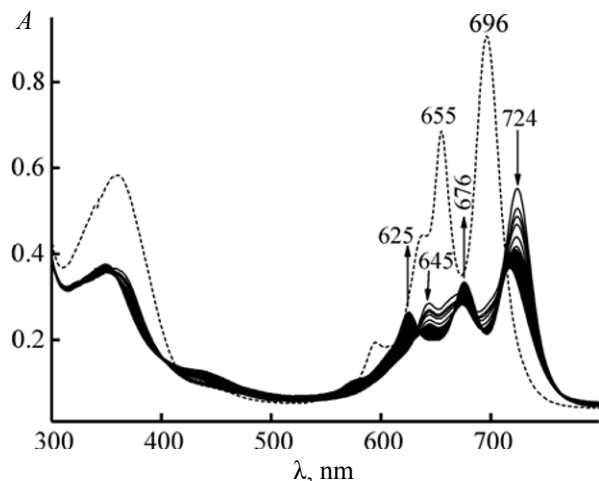


Fig. 4. Change in the electron absorption spectrum of MgDzBz₃Pz upon complex dissociation, in the benzene–acetic acid–ethanol medium [$c(\text{CH}_3\text{COOH}) = 3.50 \text{ M}$, 323 K]. (Dashed plot) shows the electron absorption spectrum of non-protonated MgDzBz₃Pz.

The observed red shift of *Q*-band in the electron absorption spectrum of H₂TTMTAP (624 → 643 nm and 557 → 568 nm) was characteristic of the protonation of *meso*-nitrogen atoms [5]. In order to

Table 5. Kinetic parameters of MgDzBz₃Pz dissociation in the benzene–acetic acid medium ($c_{\text{MgDzBz}_3\text{Pz}}^0 = 7.13 \times 10^{-6} \text{ M}$)

$c(\text{CH}_3\text{COOH})$, M	T , K	$k_{\text{ef}} \times 10^3$, s^{-1}	E , kJ mol^{-1}	ΔS^\ddagger , $\text{J mol}^{-1} \text{K}^{-1}$
0.87	298	0.16 ± 0.02^a	33 ± 2	-215 ± 10
	313	0.30 ± 0.01		
	323	0.47 ± 0.04		
	333	0.64 ± 0.01		
1.75	298	0.25 ± 0.01^a	21 ± 3	-249 ± 12
	313	0.53 ± 0.04		
	323	0.66 ± 0.03		
	333	0.86 ± 0.03		
2.62	298	0.33 ± 0.08^a	22 ± 4	-230 ± 10
	303	0.57 ± 0.01		
	313	0.79 ± 0.04		
	323	0.99 ± 0.07		
3.50	298	0.53 ± 0.03^a	22 ± 3	-241 ± 9
	303	0.87 ± 0.06		
	313	1.21 ± 0.05		
	323	1.50 ± 0.07		
4.37	298	0.67 ± 0.05^a	26 ± 2	-227 ± 12
	303	1.10 ± 0.03		
	313	1.57 ± 0.04		
	323	2.10 ± 0.08		

^a Calculated according to Arrhenius equation.

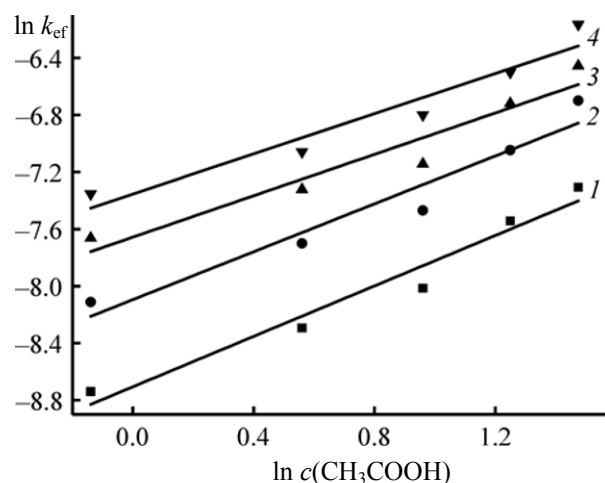


Fig. 5. Dependence of $\ln k_{\text{ef}}$ on $\ln c(\text{CH}_3\text{COOH})$ in the case of MgDzBz₃Pz dissociation at different temperatures: (1) 298 K, (2) 303 K, (3) 313 K, and (4) 323 K.

determine the number of CF₃COOH involved in the acid-base interaction, we analyzed the $\log I_i = f[\log c(\text{CF}_3\text{COOH})]$ dependence (Fig. 7). The slope of this linear plot equaled 1.74. It is known that for the media containing trifluoroacetic acid the slope values above 1 can be due to homoconjugation effect, when trifluoroacetate ion is stabilized by association with one or several acid molecules: $=\text{NH}^+ \cdots \text{OOC}(\text{CF}_3)_n$, as well as due to specific features of the porphyrizine solvation. Thus, we could not estimate the number of donor centers participating in the acid-base interaction. The stability constant of acidic form ($\text{p}K$) as determined by spectrophotometric titration equaled 2.36 ± 0.01 .

H₂DzBz₃Pz protonation was studied earlier [4] and it was shown to occur in the trifluoroacetic acid concentration range of 0–0.04 M in the CH₂Cl₂–CF₃COOH medium; $\text{p}K$ value being 2.45 ± 0.06 . However, in this case the diazepine nitrogen atom was protonated, leading to monoprotonated form, $[\text{H}_2\{\text{DzH}^+\}\text{Bz}_3\text{Pz}]$.

MgDzBz₃Pz protonation occurred via the *meso*-nitrogen atom in the CH₂Cl₂–CF₃COOH medium, at $c(\text{CF}_3\text{COOH}) = 0\text{--}1.3 \times 10^{-2} \text{ M}$ [4]. Thus, in the case of Mg complex, oppositely to the case of the free ligand, the basicity of the *meso*-nitrogen atoms of porphyrizine macrocycle was higher than that of the diazepine cycle, due to significantly ionic character of the complex. Unfortunately, the corresponding $\text{p}K$ value could not be determined because its dissociation

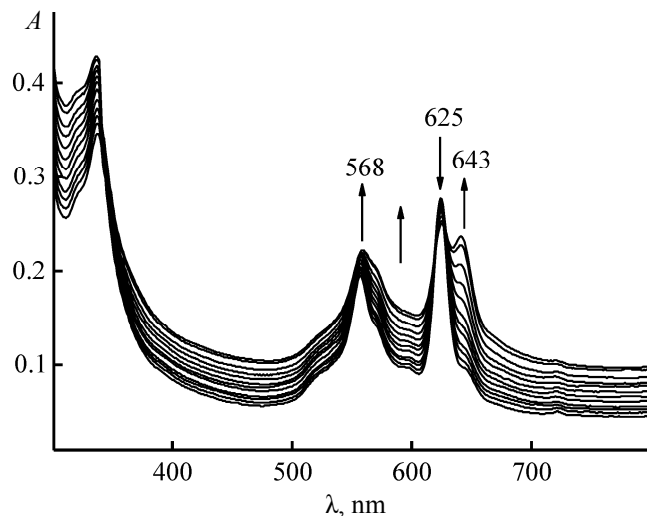


Fig. 6. Change in the $H_2TTMTAP$ electron absorption spectrum upon acid-base interaction in the dichloromethane–trifluoroacetic acid medium.

proceeding simultaneously with protonation. As H_2DzBz_3Pz basicity was higher than that of $H_2TTMTAP$ (due to the fusion of the benzene cycles with the macrocycle), the basicity of $MgDzBz_3Pz$ was, correspondingly, higher than that of $MgTTMTAP$.

$MgMATBP$ was stable in the benzene–acetic acid medium and occurred in the form with the protonated *meso*-nitrogen atom. Fig. 8 illustrates the spectral changes observed upon addition of acetic acid to the benzene solution of $MgMATBP$ at $c(CH_3COOH) = 1.75 \times 10^{-6} - 7.43 \times 10^{-4}$ M: the decrease in the absorption of the bands at 647 and 63, and the increase in the absorption of the bands at 665 and 689 nm. Such shift of the *Q*-band is typical of the protonation of the porphyrazine macrocycle *meso*-nitrogen atom [5]. The appeared acidic form was preserved in the pure CH_3COOH . In order to determine the number of CH_3COOH molecules participating in the acid-base interaction, we analyzed the $\log I_i = f[\log c(CH_3COOH)]$ dependence (Fig. 9). The slope of this linear plot was 1, which corresponded to a single donor center in $MgMATBP$ molecule. The pK value of the acidic form, as determined by means of spectrophotometric titration, equaled $+4.14 \pm 0.01$. The significant basicity of $MgMATBP$ was due to the substantial distortion of the macrocycle planar structure induced by *meso*-monoazasubstitution [6, 7], thus reducing the participation of the *meso*-nitrogen atom in the n, π -conjugation with the macrocycle. $MgMATBP$ was stable in the pure trifluoroacetic acid as well. We suggest that

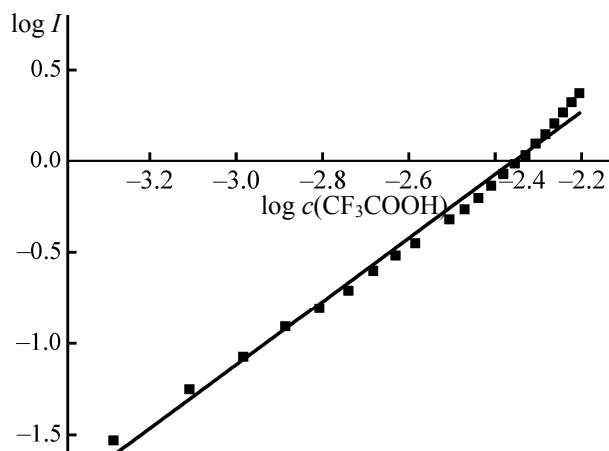


Fig. 7. $\log I = f[\log c(CF_3COOH)]$ in the case of $H_2TTMTAP$ acid-base interaction in the dichloromethane–trifluoroacetic acid medium.

benzosubstitution of the macrocycle stabilized the complex. In another study [8], the stability of Mg complex with triphenylmonoazatetrabenzoporphyrin in the benzene–acetic acid medium was investigated. It was shown that the complex was unstable and dissociated at $c(CH_3COOH) = 1.12 - 8.37$ M. Probably, the three phenyl groups at the periphery of the molecule induced its distortion and thus destabilized the complex.

Thus, $MgMATBP$ complex was the most stable in the benzene–acetic acid medium, despite of the macrocycle distortion: this complex was stable under conditions where the other complexes dissociated; the rate constants of other complexes dissociation were of the same order.

In [1], the macrocyclic effect was discussed as a tool for controlling the reactivity of tetrapyrrole macrocyclic compounds. The macrocyclic effect of porphyrins, azaporphyrins, porphyrazines, and their metal complexes is a phenomenon of atomic-electronic screening of the reactive sites H_2N_4 and MN_4 . It alters the compound reactivity via the π -electronic and structural factors. The structural part of the macrocyclic effect is characterized by the extent of the atomic-electronic screening of the reactive sites of the molecule; its effect is enhanced with the increase of aromaticity. The electronic part is determined by the efficiency of the transmission of the effect of peripheral groups to the reactive sites. The kinetic stability of the Mg complexes studied in this work was

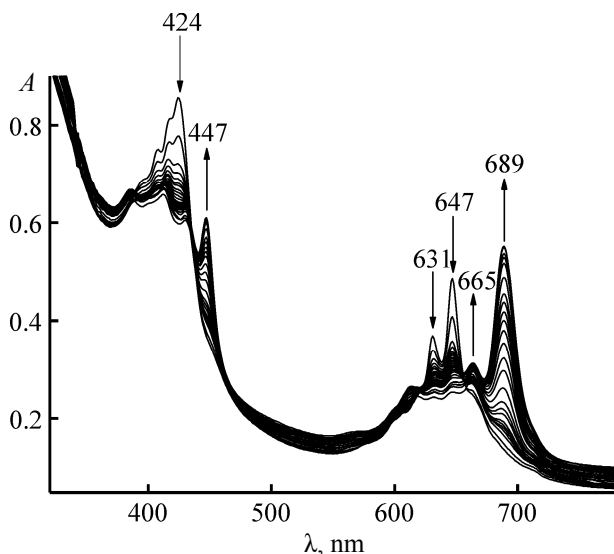


Fig. 8. Change in the MgMATBP electron absorption spectrum upon acid-base interaction in the benzene-acetic acid medium.

likely to be mainly due to the structural part of the macrocyclic effect and was due to the macrocycles aromaticity, while the effect of peripheral substituents was not that significant.

EXPERIMENTAL

Glacial acetic acid (chemically pure grade) was multiply freeze-dried and boiled with acetic anhydride. Then it was distilled (bp 118°C). Benzene was boiled at reflux above P_2O_5 for several hours and then distilled under atmospheric pressure, the intermediate fraction was collected (bp 80–81°C). Ethanol was boiled for 4 hours with calcined CaO, then CaO was separated, and ethanol was distilled (bp 78°C). Dichloromethane (chemically pure grade) was distilled under atmospheric pressure above monoethanolamine (bp 40°C).

Azaporphyrins complexes were prepared as described in [4, 9–11] and characterized by electron absorption spectroscopy and by elemental analysis.

Kinetic studies were performed in the temperature-controlled cell of Shimadzu UV-1800 photometer at varied temperature. The effective rate constant was calculated from the absorbance change at wavelengths corresponding to the bands maxima (588 nm in the case of MgTAP, 601 nm in the case of MgTTMTAP, 675 nm in the case of MgTATBP, and 645 nm in the case of MgDzBz₃) according to Eq. (7).

$$k_{\text{ef}} = 2.303/\tau[\log(A_0 - A_\infty)/A_t - A_\infty], \quad (7)$$

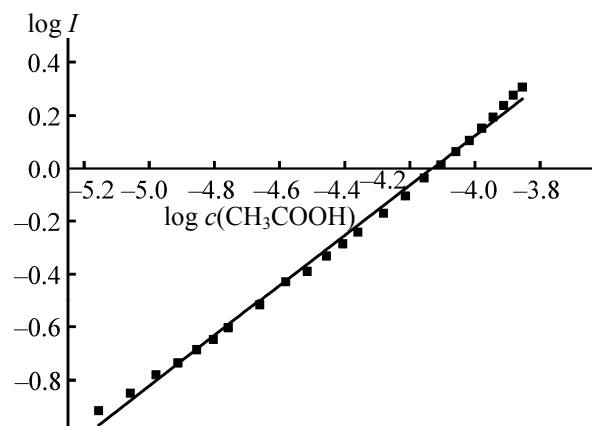


Fig. 9. $\log I = f[\log c(\text{CH}_3\text{COOH})]$ in the case of MgMATBP acid-base interaction in the benzene-acetic acid medium.

where A_0 , A_t , and A_∞ are initial, current and final solution absorbance, respectively.

For studies of acid-base interaction of MgMATBP and H₂TTMTAP, porphyrazines solutions of constant concentration were prepared in media with varied acidity, and the electronic absorption spectra were recorded with Shimadzu UV-1800 spectrophotometer at 298 K. The ratio of concentrations of acidic and basic forms at equilibrium ($I_i = c_i/c_{i-1}$) was determined from absorbance at wavelength corresponding to the acidic form absorption maximum.

The concentration stability constants of the conjugate acids in the benzene-CH₃COOH and dichloromethane-CF₃COOH media were calculated according to (8).

$$pK_i = \log I_i - n \log c[\text{CH}_3\text{COOH}(\text{CF}_3\text{COOH})], \quad (8)$$

where $I_i = c_i/c_{i-1}$ is the ratio of i th and $(i-1)$ th acidic forms concentrations in equilibrium (indicator ratio); n is the number of porphyrazine donor centers participating in the acid-base interaction in the respective stage.

MgTAP. Electron absorption spectrum (pyridine), λ , nm (log ϵ): 334 (4.60), 540 (4.14), 587 (5.07). Found, %: C 55.0; H 3.6; N 30.1. C₁₆H₈MgN₈·(CH₃OH). Calculated, %: C 55.4; H 3.3; N 30.4.

MgTTMTAP. Electron absorption spectrum (pyridine), λ , nm (log ϵ): 347 (5.00), 550 (4.26), 595

(5.12). Found, %: C 68.9; H 6.1; N 19.0. $C_{32}H_{32}MgN_8 \cdot (H_2O)$. Calculated, %: C 67.0; H 5.8; N 19.9.

MgDzBz₃Pz. Electron absorption spectrum (pyridine), λ , nm (log ϵ): 357 (4.78), 657 (4.76), 696 (4.82). Found, %: C 69.71; H 4.08; N 18.19. $C_{43}H_{24}MgN_{10} \cdot (H_2O)$. Calculated, %: C 69.69; H 3.81; N 18.90.

MgMATBP. Electron absorption spectrum (pyridine), λ , nm (log ϵ): 434 (5.02); 630; 644 (4.48). Found, %: C 75.89; H 3.40; N 12.18. $C_{35}H_{19}MgN_5$. Calculated, %: C 76.16; H 3.84; N 12.18.

MgTATBP. Electron absorption spectrum (pyridine), λ , nm (log ϵ): 653; 674 (5.11). Found, %: C 70.94; H 3.34; N 17.46. $C_{33}H_{17}MgN_7$. Calculated, %: C 73.97; H 3.20; N 18.30.

ACKNOWLEDGMENTS

This work was financially supported by the President of the Russian Federation (grant no. MK-4171.2012.3).

REFERENCES

1. Berezin, B.D., *Makrociklicheskii effekt i strukturnaya khimiya porfirinov* (Macrocyclic Effect and Structural Chemistry of Porphyrins), Moscow: Krasand, 2010.
2. Berezin, B.D. and Lomova, T.N., *Reaktsii dissociatsii kompleksnykh soedinenii* (Reactions of Dissociation of Complex Compounds), Moscow: Nauka, 2007.
3. Berezin, B.D., *Koordinatsionnaya khimiya porfirinov i ftalocianina* (Coordination Chemistry of Porphyrins and Phthalocyanine), Moscow: Nauka, 1978.
4. Donzello, M.P., Ercolani, C., Mannina, L., Viola, E., Bubnova, A., Khelevina, O.G., and Stuzhin, P.A., *Austr. Chem.*, 2008, vol. 61, p. 262.
5. Leznoff, C.C., and Lever, A.B.P. (Eds.), *Phthalocyanines. Properties and Applications*, New York: VCH Publ., 1996, vol. 4.
6. Stuzhin, P.A., *J. Porph. Phthaloc.*, 2003, vol.7, no. 12, p. 813.
7. Das, J.M., and Chaudhuri, B., *Acta Cryst.*, 1972, vol. 28, p. 579.
8. Berezin, D.B. and Shukhto, O.V., *Proc. Univ. Ser. Chem. Chem. Technol.*, 2003, vol. 46, no. 8, p. 34.
9. Linstead, R.P. and Whalley, M., *J. Chem. Soc.*, 1952, p. 4839.
10. Brown, M., Spiera, P., and Whalley, M., *J. Chem. Soc.*, 1957, p. 2882.
11. Kachura, T.F., Mashenkov, V.A., Solov'ev, K.N., and Shkirman, S.F., *Vesti Akad. Nauk Bel. SSR, Ser. Khim.*, 1969, no. 1, p. 65.